European Journal of Ophthalmology / Vol. 17 no. 2, 2007 / pp. 238-245

Retinal imaging by spectral optical coherence tomography

J.J. KAŁUŻNY[1], A. SZKULMOWSKA[2], T. BAJRASZEWSKI[2], M. SZKULMOWSKI[2], B.J. KAŁUŻNY[1], I. GORCZYŃSKA[2], P. TARGOWSKI[2], M. WOJTKOWSKI[2]

[1]Department of Ophthalmology, Collegium Medicum, Nicolaus Copernicus University, Bydgoszcz
[2]Institute of Physics, Nicolaus Copernicus University, Toruń - Poland

PURPOSE. *To demonstrate applicability of high speed spectral optical coherence tomography (SOCT) method for imaging retinal pathologies in clinical conditions.*
METHODS. *SOCT was performed in 67 eyes with different macular diseases. Examinations were carried out with the prototype SOCT instrument constructed in the Institute of Physics, Nicolaus Copernicus University, Toruń, Poland. A broadband superluminescent diode was used as a light source.*
RESULTS. *The disturbances of retinal layer structure concerning mainly outer segments of photoreceptors were observed in case of central serous chorioretinopathy and choroidal neovascularization in age-related macular degeneration. Large drusen were often related to significant changes of outer nuclear layer thickness and reflectivity.*
CONCLUSIONS. *SOCT detects small disturbances of the retinal structure and helps to precisely determine layers involved in different pathologies. (Eur J Ophthalmol 2007; 17: 238-45)*

KEY WORDS. *Spectral optical coherence tomography, Retinal imaging, Retinal layers, Central serous chorioretinopathy, Choroidal neovascularization*

Accepted: September 11, 2006

INTRODUCTION

Optical coherence tomography (OCT) is an imaging modality that enables obtaining high resolution cross-sectional reconstructions of human retina in vivo in a noncontact and noninvasive way (1). Recently this technology has been becoming a standard clinical tool for the diagnosis of a wide spectrum of ocular diseases (2-8). OCT can be applied to image either the anterior segment (9, 10) or the retina (11, 12) of human eye. OCT provides data with significantly higher resolution than other imaging modalities used in ophthalmology (13). This technology is unique in delineating the retinal layers and showing actual retinal substructure in vivo. OCT performs imaging by using optical method known as low coherence interferometry (14). This technique enables optical ranging with micrometer resolution and can be applied to semitransparent and low-scattering biological tissues. Similarly to ultrasound B-mode imaging OCT instrument first performs measurement of an axial structure of analyzed object—it collects information about the distribution of back-reflecting or back-scattering interfaces within an object distributed along a penetrating optical beam. Then the cross-sectional images are reconstructed from the set of axial measurements acquired for consecutive different positions of the penetrating beam on measured object.

Standard OCT systems, including the commercial Stratus OCT (Carl Zeiss Meditec, Dublin, CA), perform measurements using an interferometer with a mechanically scanning reference path (15). In these systems the axial structure of measured object is registered with variable time delays of the reference light beam.

1120-6721/238-08$15.00/0

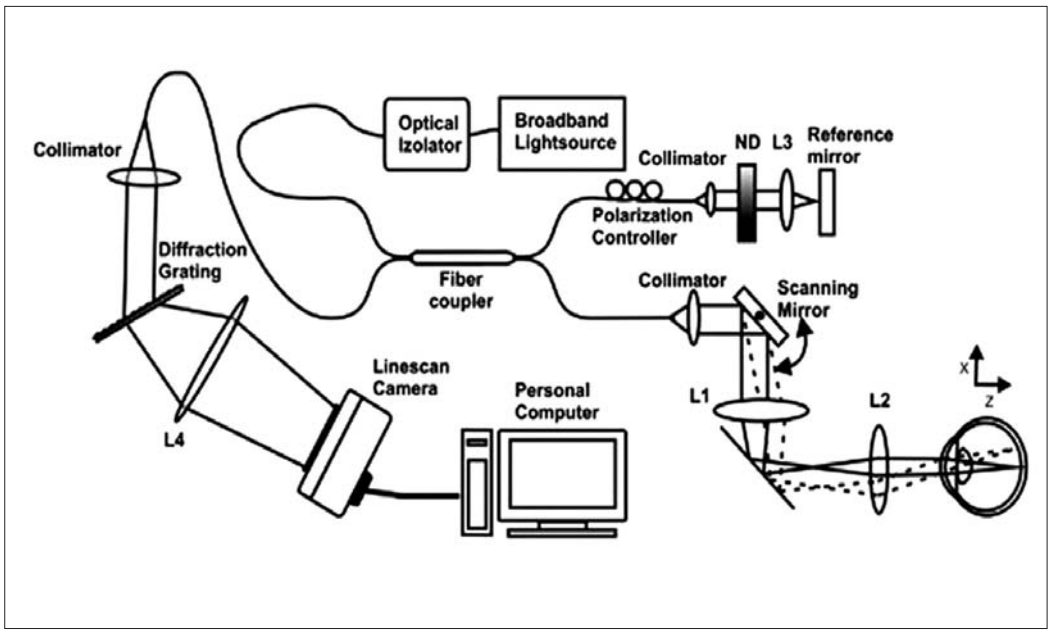

Fig. 1 - *Schematic drawing of spectral optical coherence tomography instrument: ND = neutral density filter, L1, L2, L3, L4 = achromatic lenses. Ophthalmic head consisting of collimator, lenses L1, L2, and the scanning mirror is mounted on the ophthalmic stand enabling fixation of patient head and three-dimensional manual shift of the entire head.*

Recently, an improvement of the OCT technology has been reported which enables a 50x increase in imaging speed over standard OCT systems (16-19). This new technique, called spectral OCT (SOCT), has been introduced (20-23) and commercialized as Copernicus SOCT (Optopol SA, Poland). In this technique information about axial structure of an object is obtained by measuring the interference spectrum of the light (22, 23). In contrast to standard OCT instruments the spectral OCT brings entire information about the axial structure of measured object simultaneously by parallel registration of the spectral fringe signal. Because of the parallel registration one can increase the effective illumination time of the single photodetector element. As a result, the photocurrent noise can be effectively suppressed and the sensitivity can be gained even 100 times compared to standard OCT (19, 24, 25).

The first demonstration of retinal imaging using spectral OCT was published by Wojtkowski et al in 2002 (22, 26). The first application of high-speed retinal imaging with SOCT was reported in 2003 (17, 18). Ultrahigh image resolutions of 3.5 μm in the retina with SOCT were achieved first for supercontinuum light

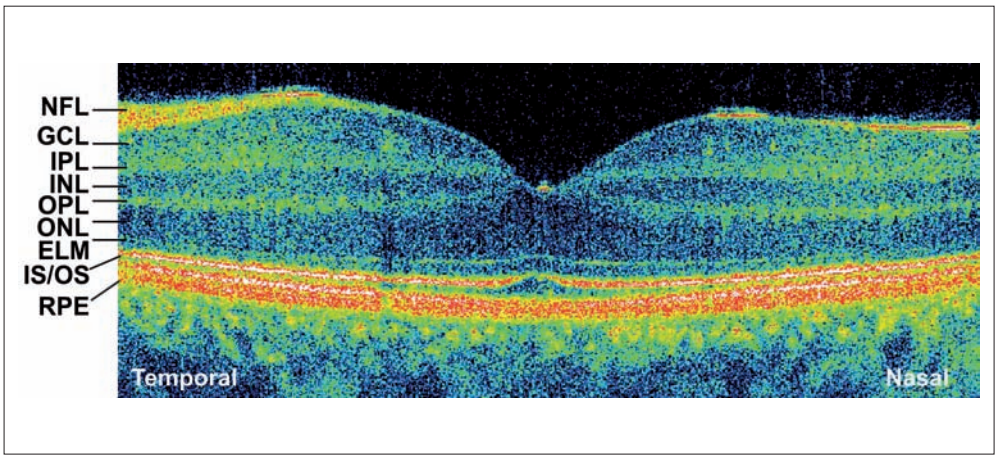

Fig. 2 - *Horizontal standard resolution spectral optical coherence tomography scan through fovea of normal, healthy retina. Intraretinal layers are labeled according to subjective correlation with retinal anatomy: NFL = nerve fiber layer; GCL = ganglion cell layer; IPL and OPL = inner and outer plexiform layers; INL and ONL = inner and outer nuclear layers; ELM = external limiting membrane; IS/OS = junction between inner and outer segments of photoreceptors; RPE = retinal pigment epithelium. The vertical scale is expanded threefold in comparison to the horizontal one.*

source (27), for broad-band semiconductor source (20), and TiSa femtosecond laser (21, 22). Applications of this novel technology for ultrahigh resolution imaging of cornea and anterior segment have been published by our group (28, 29). Demonstrations of applicability of SOCT to retinal clinical imaging were published in 2005 (30).

Due to the high sensitivity and high imaging speed of SOCT, considerable advancements in clinical studies are possible. High speed enables the collection of more information in a shorter time. It improves the quality of images, both because motion artifacts are easily avoided, and because sampling density in the image can be considerably increased. Moreover, high speed allows collection of enough data in a reasonable time to reconstruct the three-dimensional structure of an object (27, 31). In addition, a real-time examination is possible, as well as the recording of tomographic movies to unravel dynamic changes in the retina (for example, blood flow and pulsatility). The high sensitivity renders the light illuminating the eye less intense. The short exposure together with the high phase stability widens the range of measurable flows (32). SOCT also offers direct access to spectral information, which facilitates post-processing manipulations such as spectral shaping and dispersion correction (16, 33).

The purpose of this study is to demonstrate the applicability of novel high speed and high resolution SOCT based on prototype instrument constructed at Nicolaus Copernicus University for imaging retinal pathologies in clinical conditions.

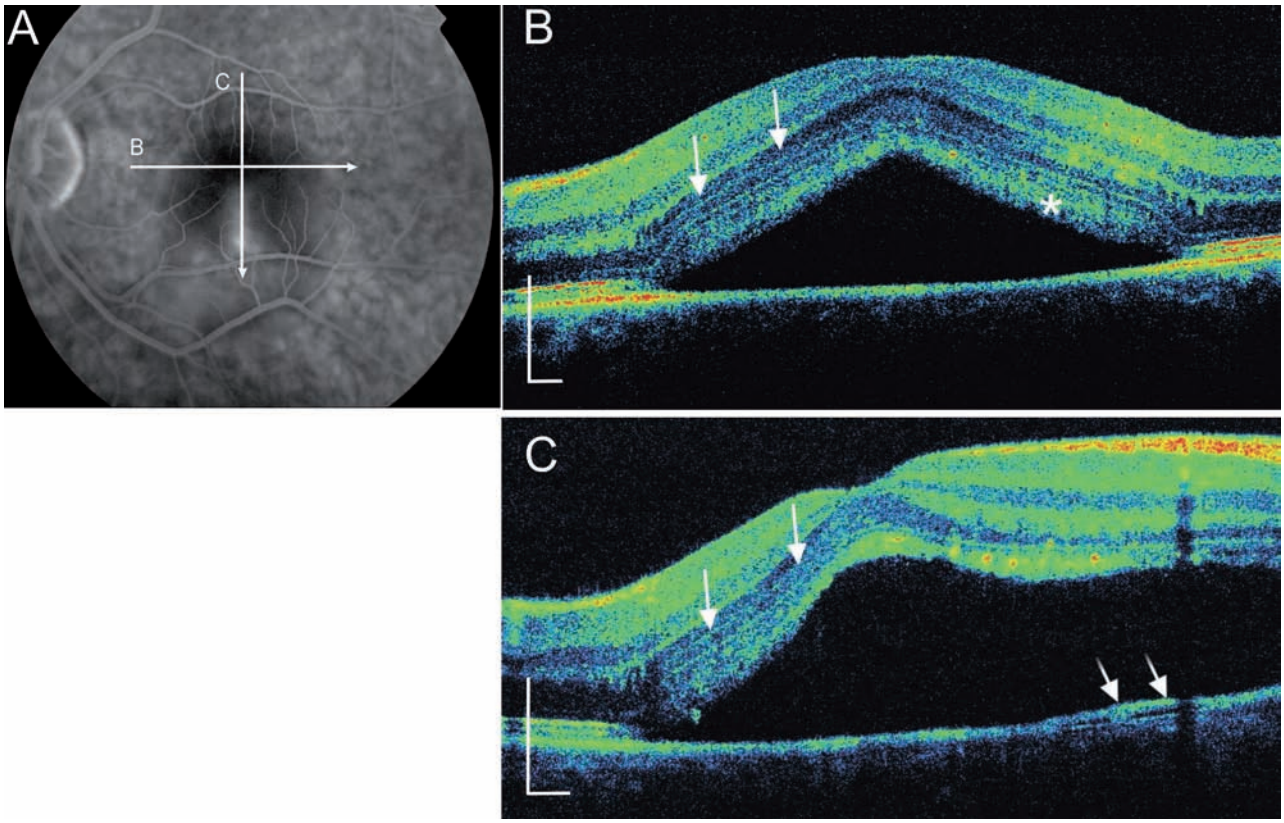

Fig. 3 - *Central serous chorioretinopathy:* **(A)** *Late phase of fluorescein angiogram shows focal leakage from choroid to the subretinal space and oval area of serous retinal detachment.* **(B)** *Spectral optical coherence tomography (SOCT) demonstrates fluid under neurosensory retina and increase of thickness and reflectivity of outer segments of photoreceptors within elevated retina (asterisk). The additional hyper-reflective line above the ELM and outer nuclear layer is marked (arrows).* **(C)** *In this sagittal SOCT scan, a small detachment of retinal pigment epithelium (RPE) with Bruch membrane can be observed (short arrows). The additional hyper-reflective line (arrows) visible in obliquely running part of elevated retina disappears in the retina parallel to the RPE. The scaling bars correspond to 250 µm.*

MATERIALS AND METHODS

Spectral OCT examinations were performed in a total sample of 44 patients (67 eyes) with the following macular diseases: central serous chorioretinopathy (CSC) (5 eyes), choroidal neovascularization (CNV) (17 eyes), macular hole (4 eyes), epiretinal membrane (6 eyes), dry form of age-related macular degeneration (20 eyes), others (15 eyes), and 4 healthy eyes without any retinal pathologies. In each case of retinal pathology, fluorescein angiography and color fundus photography were implemented (Topcon 50 TRC).
Examinations were performed with the prototype SOCT instrument constructed in the Institute of Physics, Nicolaus Copernicus University, Toruń, Poland. Figure 1 shows a schematic drawing of a spectral OCT system. Measurements are performed using a fiber-based Michelson interferometer with a low coherence length light source generated by a superluminescent semiconductor diode ($\Delta\lambda$ = 70 nm, central wavelength 830 nm). Information about the internal structure of the retina is decoded in the interference spectrum of light after passing through an interferometer with a stationary reference arm. In order to reconstruct two dimensional cross-sectional representation of the retina the probing beam is laterally scanned by the galvanometric mirrors under computer control. Additional lenses (L1, L2) help the probing beam to be introduced and scanned onto the retina without vignetting on the pupil of measured eye. The OCT instrument uses a spectrometer comprising high speed CCD linescan camera. The structural information about the reti-

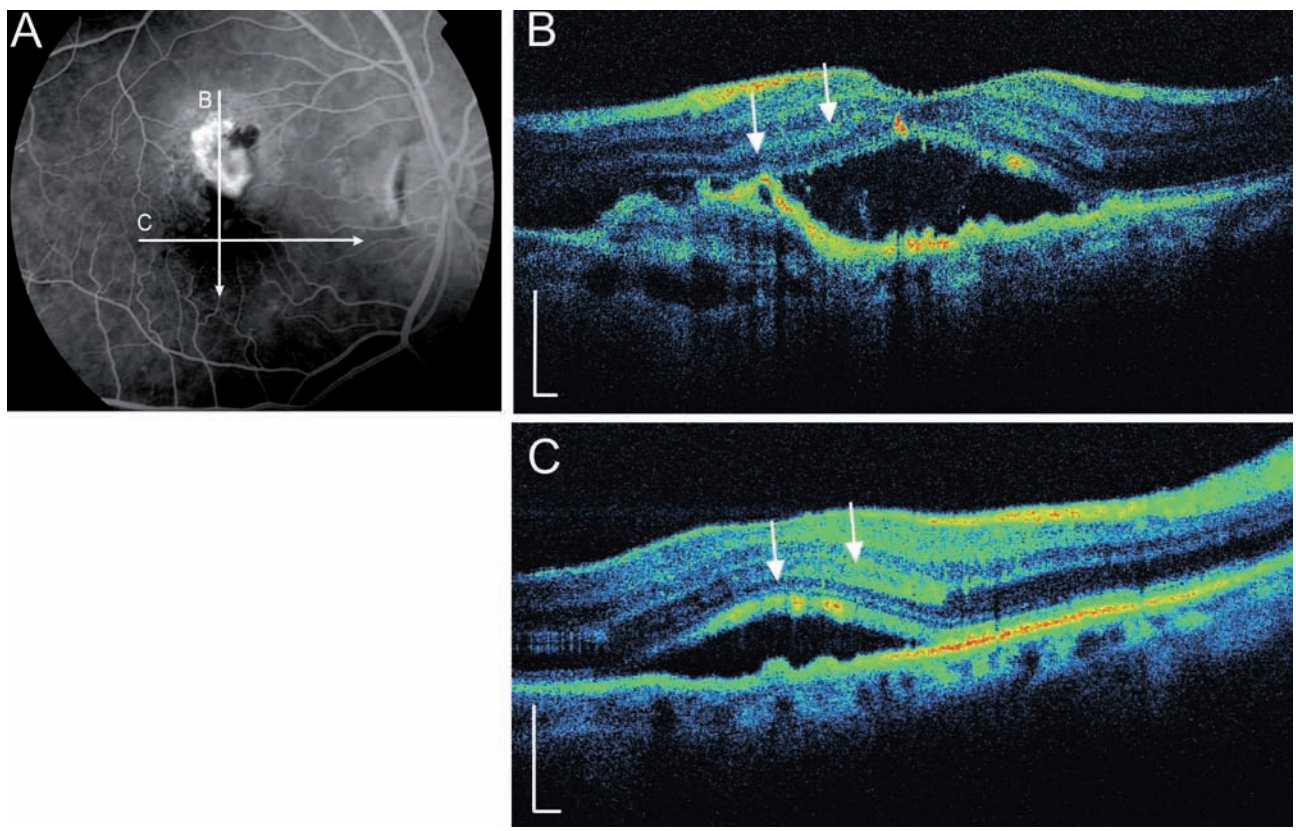

Fig. 4 - *Choroidal neovascularization (CNV) in age-related macular degeneration:* **(A)** *Fluorescein angiography shows oval area of hyperfluorescence due to CNV;* **(B)** *spectral optical coherence tomography (SOCT) demonstrates CNV under retinal pigment epithelium (RPE) and fluid under neurosensory retina. Note the thinning of outer nuclear layer (ONL) in the elevated retina close to CNV (arrows).* **(C)** *SOCT shows increase of reflectivity of outer segments of photoreceptors and within ONL (arrows). The scaling bars correspond to 250 µm.*

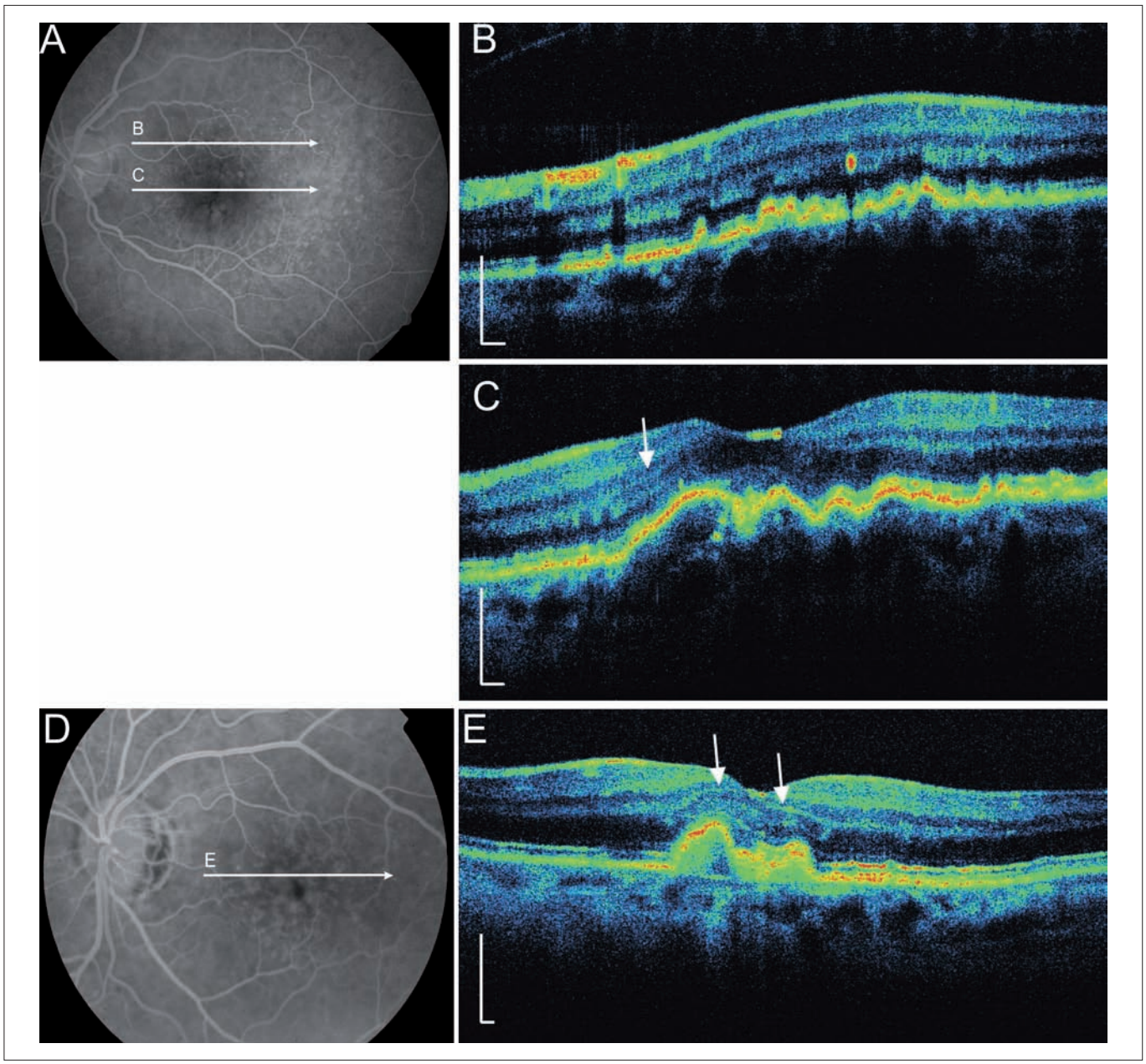

Fig. 5 - *Drusen in age-related macular degeneration:* **(A)** *Fluorescein angiography demonstrates large, confluent drusen in the fovea and small, hard drusen in the parafoveal area.* **(B)** *Spectral optical coherence tomography (SOCT) tomogram of hard drusen shows small sub-retinal pigment epithelium deposits but without changes in outer nuclear layer (ONL) reflectivity.* **(C)** *Cross-section of the fovea reveals confluent drusen and small reflectivity changes within the ONL (arrow).* **(D)** *Large soft drusen in the fovea but without leakage in the late phase of fluorescein angiography.* **(E)** *SOCT image demonstrates significant changes in ONL reflectivity above drusen (arrows). The scaling bars correspond to 250 µm.*

na is extracted using digital signal processing and Fourier Transform methods. Data acquisition speed in our system is 20,000 axial scans per second. The exposure time (during which the eye is illuminated) was 50 µs per single line of the cross-sectional image, which usually consists of 2000–5000 axial scans. Thus the total examination time was 100 to 250 ms. Length of the B-scan can be varied from 1 to 6 mm. The sensitivity of the system is 96 dB. The axial resolution of the instrument is 6 µm in air (4 µm

in tissue), while the lateral resolution is around 15 µm. The measurement head was specifically designed for posterior segment imaging of the eye, and mounted on a classical ophthalmic stand in order to perform ophthalmic imaging. The optical power of the incident beam is 750 µW at the cornea. This is consistent with European and ANSI recommended exposure limit for continuous beam viewing.

The SOCT measurements were carried out after pupil dilatation (0.5% tropicamide) with the patient in a sitting position. Neither topical application of anesthetics nor speculum insertion was necessary. Assessment of appropriate scan position was made by comparison of real time SOCT images on the monitor screen with fluorescein angiography. The correct position of the scanning beam was achieved by getting the patient to follow a fixation light or by small changes of SOCT head position. Written informed consent was obtained from all the subjects after possible consequences of the study had been explained. The study protocol was approved by the local ethics committee.

RESULTS

All important retinal layers can be delineated and recognized (Fig. 2) in SOCT cross-sectional images obtained from healthy eyes. Dark, absorbing bands correspond to nuclear layers, whereas bright, strongly reflective ones correspond to layers consisting of nerve fibers. The strong reflections in the external part of the neurosensory retina are created by the external limiting membrane (ELM), and by the junction between inner and outer segments of photoreceptors. Due to melanin accumulation, the retinal pigment epithelium (RPE) is the layer of highest reflectivity. The distance between the RPE and the junction between inner and outer segments of photoreceptors increases significantly in the foveal center because of the increased length of the outer cone segments in that region.

In the case of retinal pathologies, the regular structure of the healthy eye is disrupted. Fig. 3 demonstrates a classic case of CSC. In the SOCT image, serous detachment of the sensory retina and the presence of subretinal fluid can be observed. Compared with an unaffected flat part of the retina, the thickness and reflectivity of the outer segments of photoreceptors both increase significantly, probably due to edema (Fig. 3B). Above the ELM and outer nuclear layer (ONL), SOCT reveals an additional strongly reflecting line joining the external part of the outer plexiform layer (OPL) in unaffected areas of the retina. This feature is probably due to the border between Henle fiber layer containing obliquely running photoreceptor axons and photoreceptor cell bodies of ONL. This line is not a symptom of pathology but rather normal anatomic structure and can be observed only in the areas where scanning beam goes obliquely to the retinal surface (Fig. 3C).

In the eye with CNV secondary to age-related macular degeneration the spectral OCT images show neovascular membrane under RPE and neurosensory retinal detachment in the foveal and parafoveal regions (Fig. 4B). There is significant thinning of the ONL in the area close to the CNV. Similarly to CSC the increased reflectivity of outer segments of photoreceptors within elevated retina can be recognized (Fig. 4C).

Changes of the retinal architecture related to drusen can also be observed using SOCT. Fig. 5B presents a scan of a 64-year-old patient with small, multiple drusen which elevate the RPE and ONL. There are no changes in reflectivity within the ONL. The tomogram of the same eye going through the center of the fovea shows large, confluent drusen (Fig. 5C). In the proximity of drusen, SOCT reveals increased reflectivity of the ONL. In Fig. 5E, the scan of a patient with large, soft drusen, suspected of having CNV but without leakage in fluorescein angiography, is presented. SOCT reveals significant changes of ONL structure above the drusen but without any fluid under the RPE or neurosensory retina.

DISCUSSION

Traditional OCT has been used in clinical practice for about 10 years. Apart from fluorescein angiography and indocyanine green angiography, it is currently the most important tool in the diagnosis of macular diseases (8). This study presents our clinical experiences with a new modification of the OCT technique, SOCT, which provides images of much better quality, measured in a shorter time. The improvement in quality and resolution yields better visualization of structural changes in intraretinal layers caused by ocular pathologies. As a consequence of the high resolution, the im-

ages can be expanded threefold in the vertical direction to facilitate analysis of the retinal structure. Therefore, small disturbances of the retinal structure can be detected and a layer involved in retinal pathology can be precisely determined. The observed structural changes in CSC (Fig. 3) and CNV (Fig. 4) had been revealed previously only by ultrahigh-resolution OCT, which is more expensive and difficult to use in clinical conditions (12, 34). Our study confirms the utility of SOCT in clinical practice, and its excellent correlation with fluorescein angiography. Moreover, this method may help to reveal even very small amounts of intra- or subretinal fluid often invisible in angiographic examinations. SOCT could become an important tool in early diagnosis of CNV in angiographically doubtful cases.

ACKNOWLEDGEMENTS

Supported by Research Grant of Polish Government (2005-2008).

The authors have no proprietary interest in the publication of this report.

Reprint requests:
Jakub J. Kałużny, MD
Department of Ophthalmology
Collegium Medicum
Nicolaus Copernicus University
ul. M. Curie-Skłodowskiej 9
85-094 Bydgoszcz, Poland
kubeye@poczta.onet.pl

REFERENCES

1. Huang D, Swanson EA, Lin CP, et al. Optical coherence tomography. Science 1991; 254: 1178-81.
2. Hee MR, Izatt JA, Swanson EA, et al. Optical coherence tomography of the human retina. Arch Ophthalmol 1995; 113: 325-32.
3. Hee MR, Puliafito CA, Wong C, et al. Optical coherence tomography of macular holes. Ophthalmology 1995; 102: 748-56.
4. Hee MR, Puliafito CA, Wong C, et al. Optical coherence tomography of central serous chorioretinopathy. Am J Ophthalmol 1995; 120: 65-74.
5. Hee MR, Baumal CR, Puliafito CA, et al. Optical coherence tomography of age-related macular degeneration and choroidal neovascularization. Ophthalmology 1996; 103: 1260-70.
6. Hee MR, Puliafito CA, Duker JS, et al. Topography of diabetic macular edema with optical coherence tomography. Ophthalmology 1998; 105: 360-70.
7. Schuman JS, Hee MR, Puliafito CA, et al. Quantification of nerve fiber layer thickness in normal and glaucomatous eyes using optical coherence tomography. Arch Ophthalmol 1995; 113: 586-96.
8. Schuman JS, Puliafito CA, Fujimoto JG. Optical Coherence Tomography of Ocular Diseases, 2nd ed. Thorofare, NJ: Slack Inc, 2004; 57-483.
9. Izatt JA, Hee MR, Swanson EA, et al. Micrometer-scale resolution imaging of the anterior eye in vivo with optical coherence tomography. Arch Ophthalmol 1994; 112: 1584-9.
10. Huang D, Li Y, Radhakrishnan S. Optical coherence tomography of the anterior segment of the eye. Ophthalmol Clin North Am 2004; 17: 1-6.
11. Drexler W, Morgner U, Ghanta RK, et al. Ultrahigh-resolution ophthalmic optical coherence tomography. Nat Med 2001; 7: 502-7.
12. Drexler W, Sattmann H, Hermann B, et al. Enhanced visualization of macular pathology with the use of ultrahigh-resolution optical coherence tomography. Arch Ophthalmol 2003; 121: 695-706.
13. Drexler W. Ultrahigh-resolution optical coherence tomography. J Biomed Opt 2004; 9: 47-74.
14. Fercher AF, Mengedoht K, Werner W. Eye-length measurement by interferometry with partially coherent light. Opt Lett 1988; 13: 1867-9.
15. Swanson EA, Huang D, Hee MR, et al. High-speed optical coherence domain reflectometry. Opt Lett 1992; 17: 151-3.
16. Wojtkowski M, Srinivasan VJ, Ko TH, et al. Ultrahigh-resolution, high-speed, Fourier domain optical coherence tomography and methods for dispersion compensation. Opt Express 2004; 12: 2404-22.
17. Wojtkowski M, Bajraszewski T, Targowski P, Kowalczyk A. Real-time in vivo imaging by high-speed spectral optical coherence tomography. Opt Lett 2003; 28: 1745-7.
18. Nassif N, Cense B, Park BH, et al. In vivo human retinal imaging by ultrahigh-speed spectral domain opti-

cal coherence tomography. Opt Lett 2004; 29: 480-2.
19. de Boer JF, Cense B, Park BH, et al. Improved signal-to-noise ratio in spectral-domain compared with time-domain optical coherence tomography. Opt Lett 2003; 28: 2067-9.
20. Cense B, Nassif NA, Chen TC, et al. Ultrahigh-resolution high-speed retinal imaging using spectral-domain optical coherence tomography. Opt Express 2004; 12: 2435-47.
21. Leitgeb RA, Drexler W, Unterhuber A, et al. Ultrahigh resolution Fourier domain optical coherence tomography. Opt Express 2004; 12: 2156-65.
22. Wojtkowski M, Leitgeb R, Kowalczyk A, Bajraszewski T, Fercher AF. In vivo human retinal imaging by Fourier domain optical coherence tomography. J Biomed Opt 2002; 7: 457-63.
23. Fercher AF, Hitzenberger CK, Kamp G, Elzaiat SY. Measurement of intraocular distances by backscattering spectral interferometry. Opt Commun 1995; 117: 43-8.
24. Leitgeb R, Hitzenberger CK, Fercher AF. Performance of Fourier domain vs. time domain optical coherence tomography. Opt Express 2003; 11: 889-94.
25. Choma MA, Sarunic MV, Yang CH, Izatt JA. Sensitivity advantage of swept source and Fourier domain optical coherence tomography. Opt Express 2003; 11: 2183-9.
26. Costa RA, Skaf M, Melo LA, Jr., et al. Retinal assessment using optical coherence tomography. Prog Retin Eye Res 2006; 25: 325-53.
27. Wojtkowski M, Bajraszewski T, Gorczynska I, et al. Ophthalmic imaging by spectral optical coherence tomography. Am J Ophthalmol 2004; 138: 412-9.
28. Kaluzny BJ, Kaluzny JJ, Szkulmowska A, et al. Spectral optical coherence tomography: a new imaging technique in contact lens practice. Ophthalmic Physiol Opt 2006; 26: 127-32.
29. Kaluzny BJ, Kaluzny JJ, Szkulmowska A, et al. Spectral optical coherence tomography: a novel technique for cornea imaging. Cornea 2006; 25: 960-5.
30. Schmidt-Erfurth U, Leitgeb RA, Michels S, et al. Three-dimensional ultrahigh-resolution optical coherence tomography of macular diseases. Invest Ophthalmol Vis Sci 2005; 46: 3393-402.
31. Wojtkowski M, Srinivasan V, Fujimoto JG, et al. Three-dimensional retinal imaging with high-speed ultrahigh-resolution optical coherence tomography. Ophthalmology 2005; 112: 1734-46.
32. Leitgeb RA, Schmetterer L, Hitzenberger CK, et al. Real-time measurement of in vitro flow by Fourier-domain color Doppler optical coherence tomography. Opt Lett 2004; 29: 171-3.
33. Szkulmowski M, Wojtkowski A, Bajraszewski T, et al. Quality improvement for high resolution in vivo images by spectral domain optical coherence tomography with supercontinuum source. Opt Commun 2005; 246: 569-78.
34. Ko HK, Fujimoto JG, Schuman JS, et al. Comparison of ultrahigh and standard resolution optical coherence tomography for imaging macular pathology. Ophthalmology 2005; 112: 1922-35.